

NATIONAL AERONAUTICS AND SPACE ADMINISTRATION

Technical Report 32-1299

*A Contact Rule for Rigid-Sphere Models
of Crystal Structures*

Paul J. Shlichta

GPO PRICE \$ _____

CSFTI PRICE(S) \$ _____

Hard copy (HC) _____

Microfiche (MF) _____

ff 653 July 65

FACILITY FORM 602

N 68-30311
(ACCESSION NUMBER)

17
(PAGES)

CR-95877
(NASA CR OR TMX OR AD NUMBER)

(THRU)

(CODE)

26
(CATEGORY)

JET PROPULSION LABORATORY
CALIFORNIA INSTITUTE OF TECHNOLOGY
PASADENA, CALIFORNIA

August 1, 1968



NATIONAL AERONAUTICS AND SPACE ADMINISTRATION

Technical Report 32-1299

*A Contact Rule for Rigid-Sphere Models
of Crystal Structures*

Paul J. Shlichta

*(Now at Douglas Advanced Research Laboratories
McDonnell-Douglas Corp., Huntington Beach, Calif.)*

Approved by:

Howard E. Martens

Howard E. Martens, Manager
Materials Section

JET PROPULSION LABORATORY
CALIFORNIA INSTITUTE OF TECHNOLOGY
PASADENA, CALIFORNIA

August 1, 1968

TECHNICAL REPORT 32-1299

Copyright © 1968

Jet Propulsion Laboratory
California Institute of Technology

Prepared Under Contract No. NAS 7-100
National Aeronautics & Space Administration

Acknowledgments

The author is deeply grateful to Howard Martens, Materials Section Manager at the Jet Propulsion Laboratory, for his encouragement, and to Dr. Gerald M. Wolten, of the Aerospace Corporation, for calling the author's attention to the Russian work on topological reduction of hyperdimensional diagrams.

Contents

I. Introduction	1
II. Derivation of the Contact Rule	1
III. Two-Parameter Structures: Contact Diagrams	3
IV. Representation of Multiparameter Structures	7
A. Contour Overlap	7
B. Sections	7
C. Interfaces	7
D. Splitting of Contact Modes	9
E. Connective Skeletons	9
F. Traces of Maxima	9
G. Topological Reduction	9
H. Computer Manipulation	9
V. Extensions of the Rigid-Sphere Model	9
VI. Applications	10
VII. Conclusion	12
References	13

Figures

1. Application of contact rule to NaCl structure	2
2. Contact diagram for AlB_2 structure	3
3. Contact diagram for perovskite structure	5
4. Contact diagram for spinel structure, showing packing-fraction contours	6
5. Contacts and parameters for wurtzite structure	7
6. Overlap contact diagram for wurtzite (approx.)	8
7. Contact diagram sections for wurtzite (approx.)	8
8. Interface contact diagram for wurtzite (approx.)	8
9. Comparison of AlB_2 and $CeCu_2$ structures, showing contact-mode splitting	11

Abstract

If a crystal structure is regarded as a space-group array of rigid spheres in contact, then the relationship $F = P - C + 1$ holds, where P is the number of dimensionless variable parameters of the structure and F is the number of degrees of freedom in parameter-space when C modes of contact are present. This *contact rule* is, like Gibbs' phase rule, a simultaneous-equation rule and permits the construction of contact diagrams that show how atomic contacts change as the structural parameters are varied. These diagrams provide a convenient means of calculating and displaying the parametric variation of such properties as connectivity, coordination number, packing fraction, and the Madelung constant. To the extent that atomic radii and bond type are physically meaningful concepts, the contact rule is also useful for optimizing atomic position parameters in trial structures, comparing the bonding properties of different structures, deriving consistent values for atomic radii, and characterizing bond type.

A Contact Rule for Rigid-Sphere Models of Crystal Structures

I. Introduction

A crystal structure may be regarded as a space-group array of rigid spheres in contact; this premise underlies, for example, all usage of atomic and ionic radii. Although this model is widely used in the determination and interpretation of ionic and intermetallic structures, there has hitherto been no systematic treatment of the parametric variation of the properties of crystallographic sphere packings. It has recently been discovered (Ref. 1), however, that such structures obey the topological relation $F = P - C + 1$, where P is the number of dimensionless variable parameters in the structure and F is the number of degrees of freedom (i.e., the number of independently variable parameters) when C contact modes (sets of symmetrically equivalent contacts) are realized. This *contact rule* is analogous to Gibbs' phase rule (Ref. 2) and may be applied in similar ways, such as in the construction of contact diagrams, which show the parametric variation of the contacts and connectivity of the sphere packing. To the extent that the rigid-sphere model is a valid approximation of the real crystal structure, contact diagrams are useful for displaying or determining such properties as coordination number, packing fraction, and the Madelung constant. The contact rule may also be used to estimate optimum atomic position parameters in trial structures, to characterize bond type in a specific

structure, and to derive self-consistent sets of values for atomic and ionic radii.

This report includes a derivation of the contact rule, a description of the construction and use of contact diagrams, and a discussion of some of their advantages and limitations.

II. Derivation of the Contact Rule

A space-group array of rigid spheres may be completely described in terms of its dimensionless parameters — the $n - 1$ radius ratios of the n atomic species [differentiated either by atomic type (i.e., size) or space-group position], the unit-cell axial ratios and/or angles, and the space-group position parameters. The total number of variable dimensionless parameters for any given structure is defined as P .

The contacts between spheres fall into groups of symmetrically equivalent contacts, each such group being defined as a contact mode. Contact modes may be either homogeneous (between equivalent spheres in the same space-group position) or heterogeneous (between non-equivalent spheres or between spheres in different space-group positions).

Throughout any parametric variation of the sphere-packing, it is obvious that all contacts in a given contact mode will — because of their symmetrical equivalence — be made or broken simultaneously. At any time during such a parametric variation — that is, at any point in parameter space — the total number of operative contact modes is defined as C .

When the structure is expanded so that none of its spheres are in contact, then it possesses a degree of freedom (i.e., an independent variable) corresponding to each of its dimensionless parameters, plus an additional degree of freedom corresponding to the implicit variable of unit-cell expansion (i.e., a_0/R_n). Therefore, the total number of degrees of freedom (F) is equal to $P + 1$. If the structure is now contracted until some of the spheres come into contact, each contact mode, when present, specifies a parametric equation (i.e., the sum of the radii

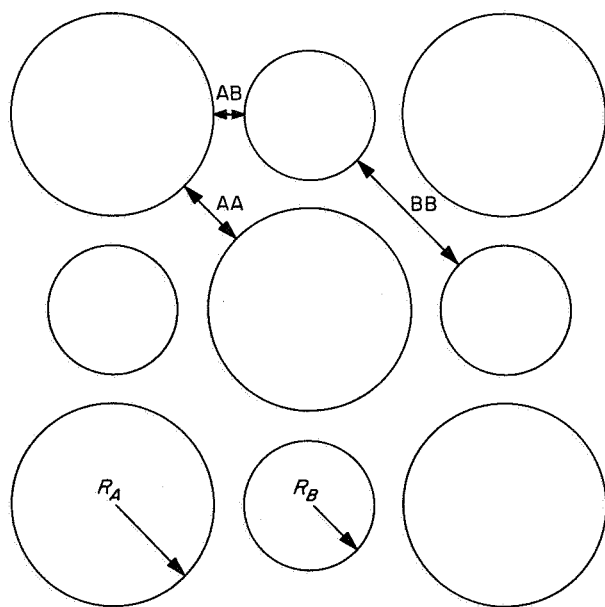
equals the distance between their centers) and thereby eliminates one of the degrees of freedom of the system. Hence, at any point in parameter space,

$$F = P - C + 1.$$

This relationship is best illustrated by considering a simple structure such as sodium chloride (Fig. 1). There is only one variable parameter, the anion-cation, radius ratio R_A/R_B , but there are three possible contact modes: AA and BB, both in the $\langle 110 \rangle$ direction, and AB in the $\langle 100 \rangle$ direction. According to the contact rule, we can make the following statements:

- (1) The presence of only one contact mode permits one degree of freedom; e.g., AB contact is possible for any value of R_A/R_B between 0.414 and 2.415.

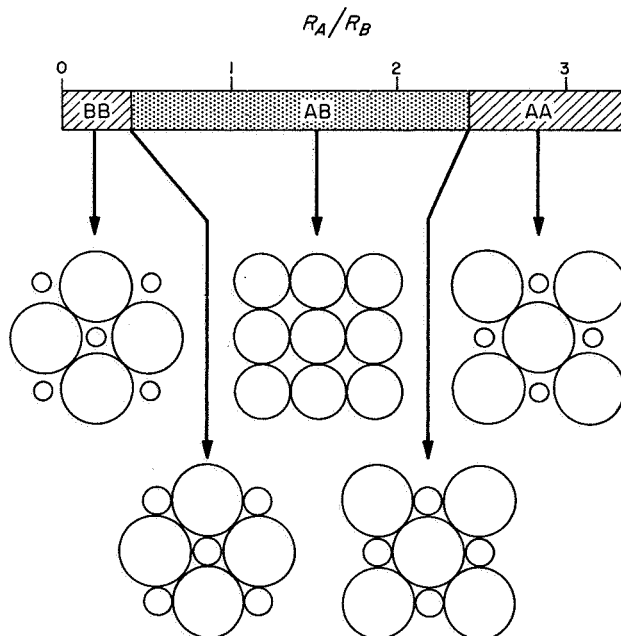
CONTACTS AND PARAMETERS



$$F = P - C + 1$$

$$P = 1, \text{ OR } R_A/R_B$$

CONTACT DIAGRAM



CONTACTS	VALUE		
	C	F	R_A/R_B
AB	1	1	0.414 TO 2.415
AA, AB	2	0	2.415
AA, AB, BB	3	-1	IMPOSSIBLE

Fig. 1. Application of contact rule to NaCl structure

- (2) Two simultaneous contact modes permit no degrees of freedom, so the structure is completely specified; e.g., simultaneous AA and AB contact fix the radius ratio at 2.415.
- (3) It is impossible to have all three contact modes present simultaneously.

These conclusions may be verified by geometric construction, as shown in Fig. 1.

III. Two-Parameter Structures: Contact Diagrams

The contact rule, like Gibbs' phase rule, is a special case of the simultaneous-equation rule¹ that, in turn, is equivalent to the topological tiling theorem of Lebesgue and Brouwer (Ref. 3). For this reason, any application of the contact rule to a specific structure type automatically implied the existence of a contact diagram in

¹Despite an apparent similarity in external form, and despite several claims to the contrary, these rules have no relation or analogy to Euler's rule for polyhedra (Ref. 4).

parameter space. For a two-parameter structure, for example, each domain of the two-dimensional contact diagram corresponds to the range of parametric values in which one contact mode is operative, each boundary between two domains corresponds to the values for which two contact modes (of the two adjacent domains) are simultaneously operative, and each triple point (i.e., the meeting point of three domains) corresponds to the unique values for which three contact modes are simultaneously operative. This is illustrated for the AlB_2 structure-type in Fig. 2.

A contact diagram may be constructed in the following manner:

- (1) By inspection of the structure, all possible contact modes are identified and a contact equation, e.g.,

$$(R_A + R_N)^2 = (X_A - X_N)^2 + (Y_A - Y_N)^2 + (Z_A - Z_N)^2$$

is identified with each contact mode.

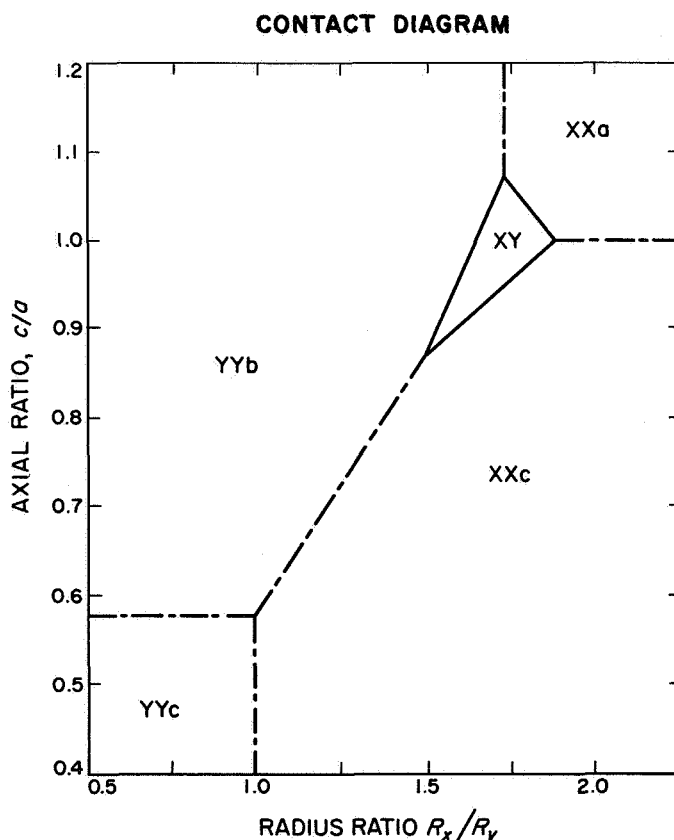
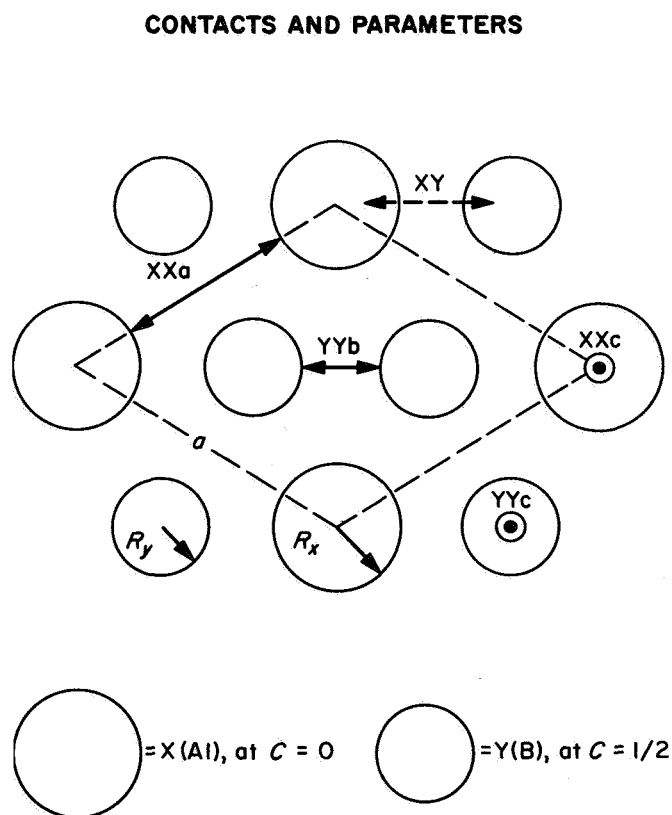


Fig. 2. Contact diagram for AlB_2 structure

- (2) All possible triple points are determined by finding simultaneous solutions for all possible combinations of three contact equations. Solutions having unrealistic values for the parameters (e.g., negative or imaginary values) are discarded.
- (3) The remaining triple points are compared with the original structure by inspection or by geometric construction. Points that are not physically realizable (e.g., those which require interpenetration of spheres) are discarded.
- (4) The remaining triple points are plotted on the contact diagram. By means of the contact equations, connecting boundary lines are calculated and plotted between all pairs of triple points having two contact modes in common.

A more formal and general program for calculating contact diagrams will be discussed in Section IV.

Properties that depend only on the number and types of contact modes, such as lattice connectivity and coordination number, have constant values within each contact mode domain and along the boundaries between them. They may, therefore, be readily mapped on the contact diagrams by appropriate labeling.

Connectivity, the incorporation of all the spheres in the structure into a continuous contact-network such that a path of contacts exists between any two spheres in the structure, may be determined in simple structures by inspection. Fischer (Ref. 5) has an elegant method of determining connectivity in homogeneous sphere packings, i.e., packings of single crystallographic complexes. Each contact mode is identified with the symmetry operation (or operations) which transforms a position from one end of a contact to the other. If, at any given point in parameter space, the set of symmetry operations corresponding to the operative contact modes is sufficient to generate the complete symmetry group of the space-group, then the structure is connective at that point. An analogous, though more complex, rule undoubtedly exists for heterogeneous sphere packings.

The connective regions in a contact diagram correspond to entire contact-mode domains and/or the entire boundaries between them; these may be designated by shaded areas, solid lines, and circled triple points. In the AlB_2 structure, for example, XY contact is both a necessary and sufficient condition for connectivity (Fig. 2). In the idealized perovskite structure, however, only the AC + BC and AC + AB boundaries are connective

(Fig. 3). Since connectivity is usually a requirement in any real structure, the connective regions of the contact diagram will usually be the only physically meaningful regions. Apparent exceptions, however, such as LiI and Cu_2O , do exist.

Coordination number — taken in the strict sense as the number of spheres in contact with a given sphere — can be determined readily from the multiplicity of the contact modes, i.e., the number of contacts per unit all belonging to a given contact mode. If, for the structure A_xB_y , X_A is the number of A spheres per unit cell and M_{AAi} and M_{ABj} are the multiplicities of the i^{th} AA (homogeneous) mode and the j^{th} AB (heterogeneous) mode, respectively, then the coordination number K_A at any given point is given by:

$$K_A = \frac{2 \sum_i M_{AAi} + \sum_j M_{ABj}}{X_A}$$

This relation is illustrated in the contact diagram in Fig. 3. The notation used is somewhat redundant; only the multiplicities need be listed. Needless to say, for a given species, the coordination number at a boundary or triple point is the sum of the coordination numbers in the adjacent domains.

Other properties that also depend on the sphere-packing characteristics of the structure, such as packing fraction and the Madelung constant (Ref. 6), have values that vary within any one contact domain. In such cases, the contact diagram serves as a convenient matrix for the calculation and representation of these properties. Within each domain, the equation that determines the quantity in question is derived from the contact equation of that domain. The values of the quantity are most conveniently represented as contour lines within the contact domains. These contour lines are continuous across the domain boundaries, but their derivatives are discontinuous at the boundaries; this property illustrates how much more difficult it would be to compute these quantities without the aid of contact diagrams.

A typical calculation of contour lines of packing fraction (the volume percentage of space filled by spheres) is shown in Fig. 4. Whereas packing-fraction calculations are exact, calculations of the Madelung constant are only approximate because they assume a rigid-sphere model — that is, an infinite exponent in the repulsive energy term. The possibility of refinements involving a soft-sphere model will be discussed in a later section.

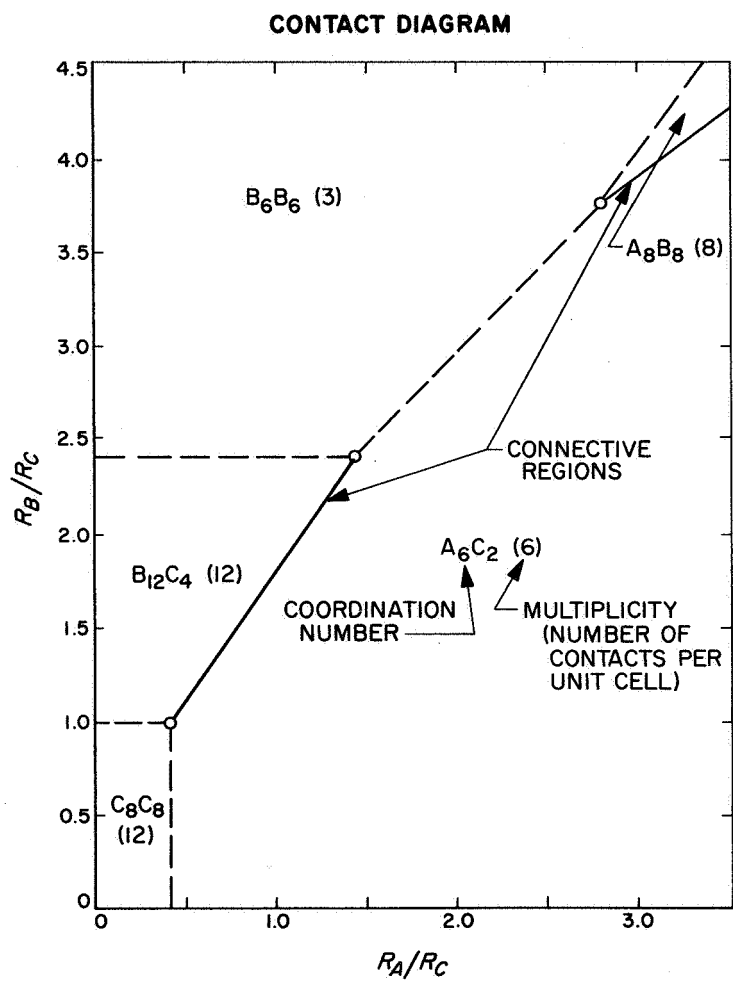
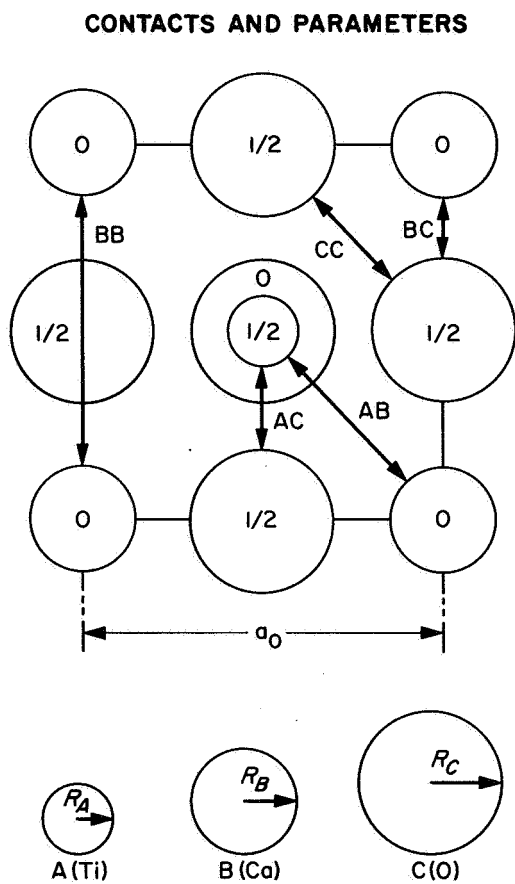
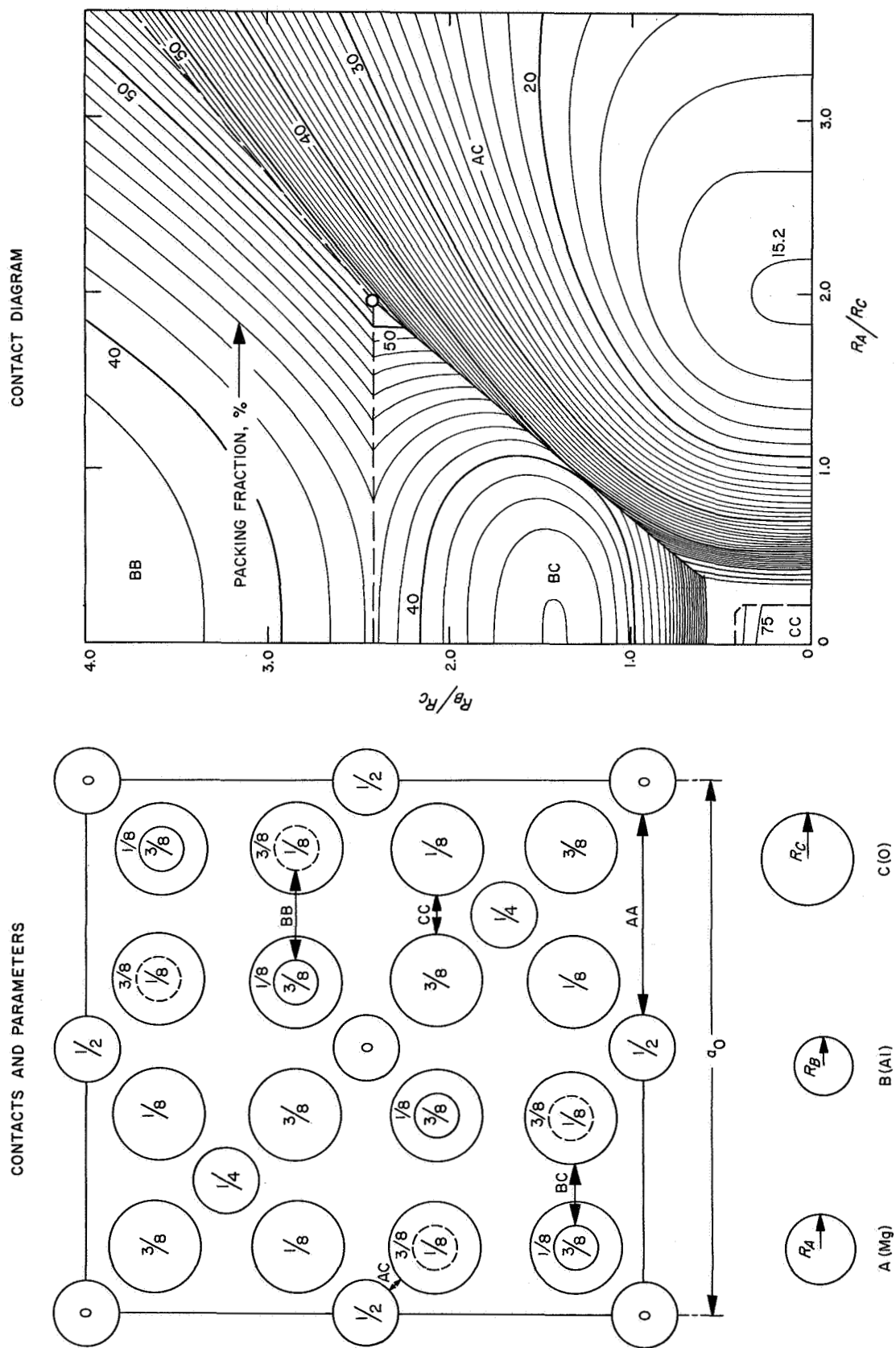


Fig. 3. Contact diagram for perovskite structure



IV. Representation of Multiparameter Structures

The advantages of contact diagrams for two-parameter structures have, it is hoped, been amply demonstrated. Unfortunately, most structures of interest have far more than two or three parameters, so their contact diagrams would have to be constructed in hyperspace. This necessity constitutes the chief limitation of the contact rule at this time. Before widespread application is possible, it will be necessary, first, to develop a generalized program for computing multiparameter contact diagrams and, then, to devise suitable means for representing these hyperspace diagrams in usable and comprehensible form.

At present, two computer programs for the calculation of sphere contacts are being developed. The author is attempting to construct a matrix program for solving the contact equations of any structure with ten parameters or less. This method, however, presupposes the prior selection of contact modes and the formulation of the contact equations, which, at present, is done by inspection. However, it is possible that a group-theory formalism can be developed that will simplify this part of the problem. On the basis of different premises, Fischer (Ref. 5) is developing a program for calculating the sphere contacts in homogeneous sphere packings (packings of a single lattice complex). In his method, the possible contact between each pair of points in the complex is calculated separately. Presumably, the family relationship between contacts in the same contact mode will then be identified by their identical parametric variation. Although both programs have their difficulties and disadvantages — in both cases, for example, heterogeneous packings are far more difficult than homogeneous ones — the problems are by no means unprecedented and it may safely be assumed that workable programs for computing contact diagrams will be available in the near future.

On the other hand, the problem of representing or displaying a hyperdimensional contact diagram in a convenient and usable form is much more difficult. No ideal solution exists (short of transforming crystallographers into hyperspace beings), and different applications will probably require different methods. Some fairly successful techniques have already been developed by metallurgists for the interpretation of multicomponent phase diagrams. Other methods are peculiarly applicable to contact diagrams because, as a rule, only a very restricted portion of any one diagram is of practical interest, i.e., the connective regions lying in zones of radius ratios or axial ratios in the range of those observed in real structures.

The following methods constitute only a partial and tentative list of techniques that might be of value.

A. Contour Overlap

A three-dimensional structure may obviously be represented in two dimensions by a stereophotograph of a three-dimensional model. This effect may also be achieved, in part, by the use of overlapping shaded areas. An example of such a diagram is shown in Fig. 6 for the wurtzite structure, whose parameters and contact modes are shown in Fig. 5. This method is only useful for fairly simple three-parameter structures.

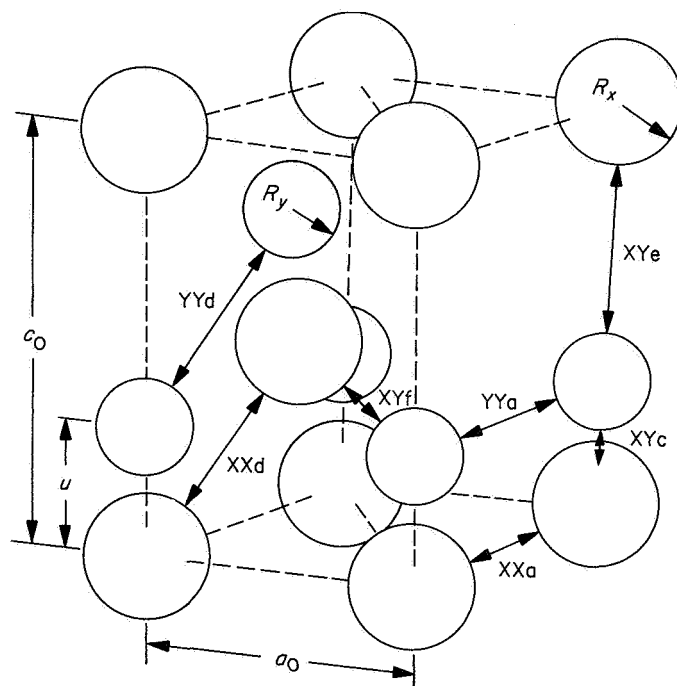


Fig. 5. Contacts and parameters for wurtzite structure

B. Sections

A series of two-dimensional diagrams (for which all but two parameters are held constant) can be constructed and viewed in sequence. This is illustrated for the wurtzite structure in Fig. 7. If the contact diagram of a three-parameter structure is sufficiently simple, a series of sectional views, in which one parameter is varied systematically, can be superimposed; the result is similar to a contour map.

C. Interfaces

If two or more contact modes are arbitrarily equated, the resultant contact diagram will completely include the

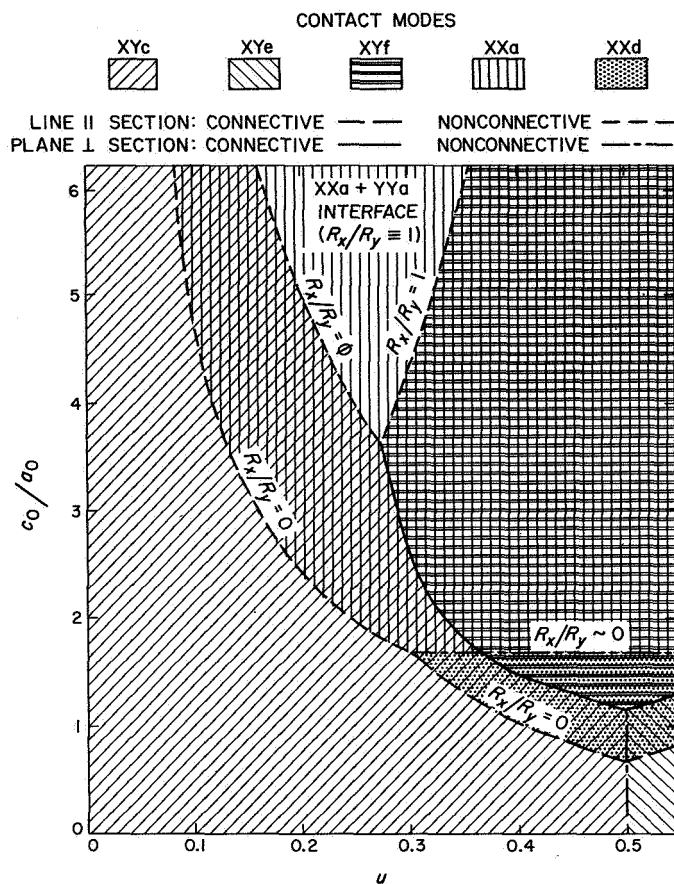


Fig. 6. Overlap contact diagram for wurtzite (approx.)

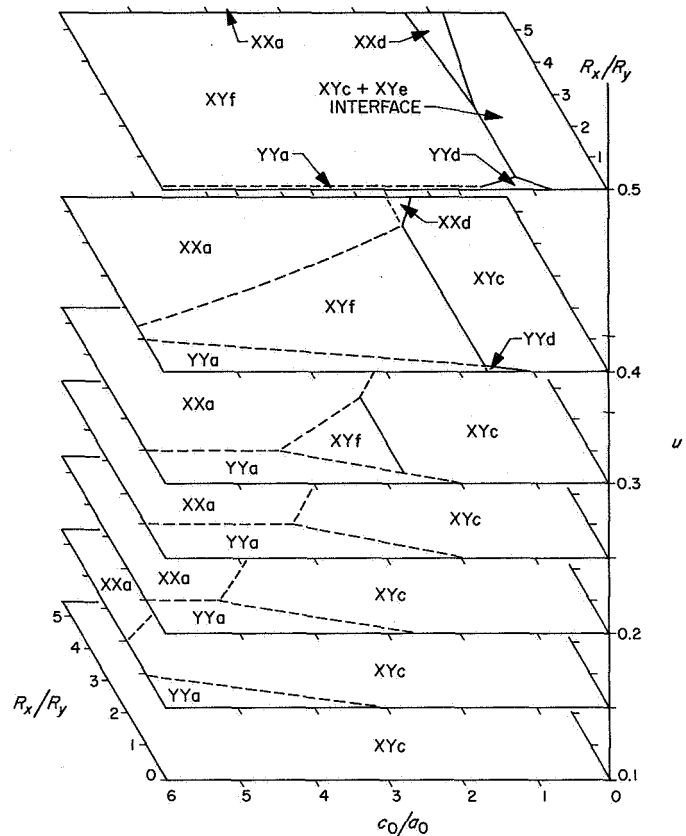
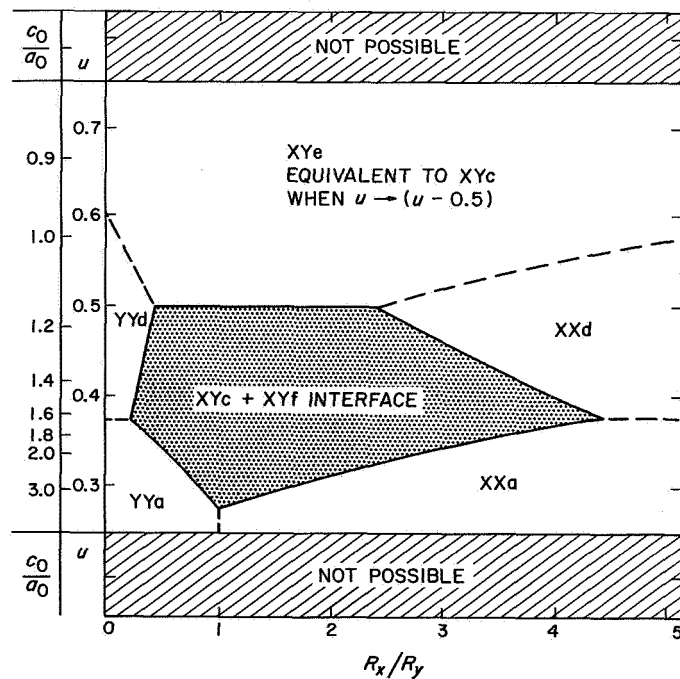


Fig. 7. Contact diagram sections for wurtzite (approx.)

$$XYc \equiv XYf \quad \frac{c_0}{a_0} = 1/\sqrt{3} (u - 1/4)$$

Fig. 8. Interface contact diagram for wurtzite (approx.)



boundary common to the domains of all the equated contacts. An example of such a diagram for the wurtzite structure is shown in Fig. 8.

D. Splitting of Contact Modes

If the multiparameter structure is a distortion of a simple structure of higher symmetry, then, as the parameters are varied from the symmetrical to the distorted structure, the contact modes may be thought of as splitting into nonequivalent subgroups. Figure 9 illustrates this case for the distortion of the AlB_2 structure to the $CeCu_2$ structure. It will be noted, for example, that the XXa mode splits into (1) the $XXas$ mode, which contracts; (2) the $XXas$ mode, which expands; and (3) the $XXan$ mode, which remains approximately the same. Therefore, it may be inferred that, in the $CeCu_2$ structure, the $XXas$ mode is the most important of the three. Further, one may, by inspection only, infer that the combination $XYa + XYb + XYc + XYd + YYcs + YYbb + XXas$ is likely to be a significant septuple-point in the $CeCu_2$ contact diagram.

E. Connective Skeletons

As was mentioned earlier, the regions of interest in a contact diagram are usually restricted to the connective portions of the diagram. It is reasonable to expect that, in a multiparameter structure, no single contact-mode domain will be connective; rather, one expects that connectivity will be confined to boundaries common to several domains and, therefore, of lower dimensionality. For example, in a structure with n different species of spheres, a connective region must simultaneously adjoin at least $n - 1$ contact-mode domains. In at least some cases, the connective regions may form a skeleton-like framework of connected lines, surfaces, and/or volumes in real space. If so, a model of the connective skeleton could be constructed and labeled at intervals with the corresponding sets of hyperdimensional coordinates. With sufficient study, such a skeleton model might convey considerable information about the structure.

F. Traces of Maxima

An even more restricted, and possibly more meaningful, representation of the contact diagram would be a skeleton (or rather network) of traces of packing-fraction or the Madelung constant maxima of the diagram. In nonconnective regions, these would be the one-dimensional

n -fold boundaries²; in the connective regions, the skeleton could be defined as the trace of the least steep descent from the maximum. The labeling at suitable intervals along each member of the network would include the set of coordinates (parameter values) plus the value of the packing fraction or the Madelung constant at that point. Such a skeleton should, with practice, be quite easy to interpret. This method may have some analogy to the *packing map* method used by Samson (Ref. 7) for the solution of complex intermetallic structures.

G. Topological Reduction

Contact diagrams are, by definition, divisions of n -dimensional space into polytopes, all of whose zero-dimensional vertices adjoin exactly $n + 1$ domains. For this reason, they are subject to certain topological reductions and projections which, it is claimed, are of great value in interpreting multicomponent phase diagrams (Refs. 8, 9, and 10). Since contact diagrams tend to be considerably simpler than phase diagrams of the same dimensionality, it is reasonable to assume that these same techniques will be of value in the interpretation of multiparameter contact diagrams.

H. Computer Manipulation

In the long run, the most practical method may be simply to store the entire contact diagram in the computer in such a form that, upon command, any section, interface, connective skeleton, or trace of maxima is available for immediate display. Such systems are already in use for solving engineering problems (Ref. 11), and an application to contact diagrams should not be difficult.

To date, none of these techniques has been seriously tried, and it will undoubtedly be several years before their relative efficacy can be evaluated.

V. Extensions of the Rigid-Sphere Model

Thus far, the contact rule has been applied only to structures composed of rigid spheres of coordination-invariant size. It is possible to consider other models that correspond more closely to real atoms and crystals. Each of these variations, however, entails additional complications and difficulties.

²Throughout the nonconnective regions of a contact diagram, the points of maximum contact always correspond to packing-fraction maxima; this is not necessarily true, however, within the connective regions.

For example, the rigid spheres might be replaced by soft spheres whose repulsion potential has a finite exponent. The gross effect of this modification on the contact diagram would be to blur the boundaries between contacts or to give them a finite thickness. This would be a considerable refinement in the calculation of the Madelung constant contour lines and might even be advantageous in the optimization of packing fraction in ideal metallic structures. To calculate contact diagrams from this model, however, it is necessary to specify the attractive potential, also. This would make the diagram less general and would involve considerably greater difficulty in computation. Therefore, before using this model in the computation of the Madelung constants, for example, it would be wise, first, to use the rigid-sphere model and, then, compare it at representative points with the more precise calculations to see if the discrepancy is worth the extra effort.

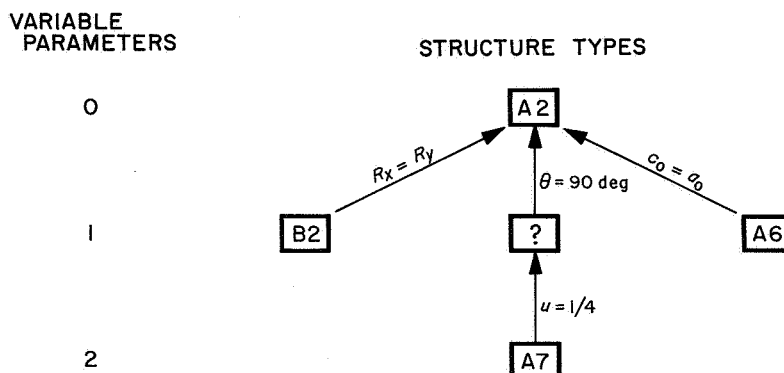
A more serious limitation of the current model exists in its application to intermetallic structures. It is generally agreed, on the basis both of elementary theory and empirical correlation, that the radius of a metallic atom increases with increasing coordination number (Refs. 12 and 13). It can be demonstrated readily that, if the contact diagram is plotted in terms of *standard metallic radii* (estimated for constant coordination or extrapolated to zero coordination), the coordination-variations of the radii cause the contact domains to overlap each other, with the contact boundaries lying somewhere in the regions of overlap. However, this seeming inconsistency appears to be easily resolvable; it may even provide a means of estimating the variation of effective coordination with near-contact proximity of other atoms. In this event, coordination numbers could no longer be regarded as strictly constant throughout a contact domain,

and contour lines would have to be used — at least in the regions of apparent overlap.

Finally, it would be hypothetically possible to replace the spheres by other geometric solids such as ellipsoids or polyhedra. However, this substitution is, in practice, quite infeasible, not only because there is no good reason for doing it, but because it would worsen that aspect of the contact diagram that already causes the most difficulty — its hyperdimensionality. A sphere can be specified by only one nonpositional parameter, i.e., its diameter. An ellipsoid of revolution requires three additional parameters — one axial ratio and two orientation angles. General ellipsoids and nonregular polyhedra would require even more additional parameters. It is unlikely, therefore, that this modification of the contact rule will ever be used.

VI. Applications

As an aid to the study and interpretation of crystallographic sphere packings, the contact rule is of considerable usefulness and entails no approximations or inaccuracies. By way of trivial example, it is an excellent way of determining optimum cork-ball sizes for sphere-packing models of crystal structures. In any program for deriving all possible binary sphere packings — as might be done, for example, by combining Fischer's computation of homogeneous complex sphere packings (Ref. 5) with Biedl's *stuffing sphere* program (Ref. 14) — the contact rule would serve, at the very least, as a convenient method of representation of these systems. In addition, the contact rule is uniquely suitable for deriving parametric *family trees* for showing relationships between distorted forms of a parent structure. One example of this is given in Fig. 9, another is shown below:



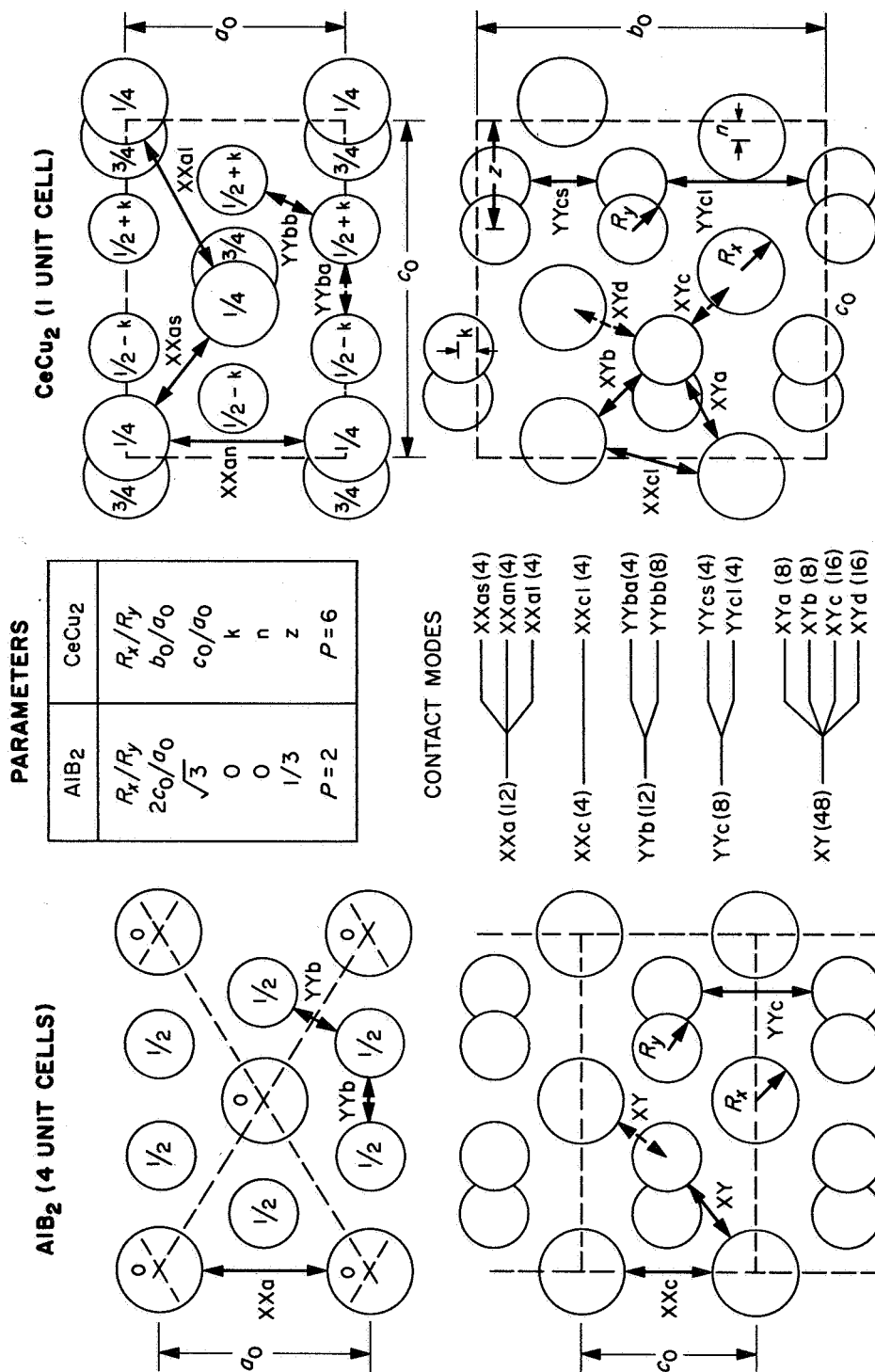


Fig. 9. Comparison of AlB₂ and CeCu₂ structures, showing contact-mode splitting

This method is complementary to, and in some cases, an improvement over, existing structural classifications. These relationships can be studied easily or displayed quantitatively, since the contact diagram of any structure in such a tree is a section or interface of the contact diagram of the structure beneath it.

On the other hand, any applications of the contact rule to specific structures or compounds must be handled with discretion. It must always be borne in mind that the contact rule is not a law of chemistry or physics but merely of geometry; it does not apply to real compounds but only to one simplified – albeit widely used – model of them.

With this restriction in mind, the contact rule may be used for the interpretation of structural parameters in terms of bond type and empirical atomic radii. Ideal metallic or ionic bonding, for example, can be approximated legitimately by rigid spheres held together by nondirectional forces. We might, therefore, assume that structural optimization of metallic structures would imply both connectivity and a maximization of packing fraction. Ionic structures would tend to be optimized near the Madelung constant maxima, lying presumably in connective regions. Covalent bonding, however, is highly directional and permits a continuous range of bond distances with no specifiable *contact distance*. Therefore, neither the concept of atomic radii nor the contact rule applies to covalent structures, and these cannot be assigned to any specific position on a contact diagram.

These criteria may be illustrated by typical AlB_2 type structures. On the basis of the contact diagram (Fig. 2) we might presume that ideal metallic compounds would be optimized within the XY domain, perhaps near the triple points. Presumably, ideal ionic structures would be favored by a maximum of anion-cation contacts and an avoidance of homogeneous contacts; hence, these compounds might be optimized near the center of the XY domain.

If we now consider the compounds having the AlB_2 type structure, one group [$CeGa_2$, $LaGa_2$, etc. (Ref. 15)] all have a c_0/a_0 axial ratio of approximately 1.0. If con-

ventional metallic radii (Ref. 13) are assumed, these structures would lie deep in the nonconnective region of the YYb field of the contact diagram; this fact suggests that these structures are not ideally metallic. If we assume some degree of ionic character, the gallium with a partial positive charge, the radius ratio R_x/R_y would increase and the position of these structures on the contact diagram would shift toward the center of the XY field, a location consistent with the postulate of ionic character. In contrast, the transition metal borides, such as ZrB_2 and WB_2 (Ref. 16), have c_0/a_0 axial ratios greater than 1.1, so that it is impossible to place these structures on a connective portion of the AlB_2 contact diagram. Therefore, these structures are probably predominantly covalent.

Similar procedures, applied to the contact diagram of a structure type representing a large number of ionic compounds (e.g., spinel), might lead to the derivation of a set of self-consistent ionic radii. These techniques may also be of value in optimizing parameters of trial structures in X-ray diffraction structural determinations.

Finally, the contact rule may provide some philosophical insights into the reasons which cause a given chemical compound to *choose* one structure type in preference to another. For one thing, the contact rule does not imply that all the densest sphere packings are necessarily of high symmetry. As the symmetry is lowered and the number of parameters increases, the contact modes do indeed split into modes of lower multiplicity, but the allowed number of simultaneous contact modes also increases. Therefore, a low-symmetry multiparameter structure may have a connectivity and density comparable to its high-symmetry analog (cf. Fig. 9).

VII. Conclusion

This report has been intended to demonstrate that the contact rule and contact diagrams have unique advantages in the study of sphere-packing models of crystal structures. The actual extent of their usefulness, however, remains to be determined. To this end, work is now in progress on the application of contact diagrams to crystal chemical investigations of simple ionic structures.

References

1. Shlichta, P. J., *Bull. Am. Phys. Soc.*, Ser. II, Vol. 9, No. 7, p. 742, 1964; and *International Union of Crystallography, Seventh Congress (Moscow): Abstracts*, p. 34, 1966.
2. Findlay, A., *The Phase Rule and Its Applications*. Dover Publications, Inc., New York, 1951.
3. Courant, R., and Robbins, H., *What is Mathematics?* p. 251. Oxford University Press, London, 1941.
4. Shlichta, P. J., *Bull. Am. Phys. Soc.*, Ser. II, Vol. 12, No. 8, p. 1142, 1967.
5. Fischer, W., *International Union of Crystallography, Seventh Congress (Moscow): Abstracts*, p. 52, 1966.
6. Kittel, C., *Introduction to Solid State Physics*, 2nd ed., 72 ff. John Wiley & Sons, Inc., New York, 1956.
7. Samson, S., *Am. Crystallog. Assn.: Program and Abstracts (Minneapolis)*, p. 57, 1967.
8. Paletnik, L. S., and Landau, A. I., *Dokl. Akad. Nauk SSSR*, Vol. 10, p. 954, 1956; *Zh. Fiz. Khim.*, Vol. 31, p. 304, 1957; and *Sbornik Trudov, Khim. i Tekhnol. Silikatov*, p. 79, 1957.
9. Perelman, F. M., *Zh. Neorg. Khim.*, Vol. 3, p. 630, 1958.
10. Lambin, L. N., and Ermolenko, N. N., *Zh. Prikl. Khim.*, Vol. 32, p. 548, 1959.
11. Eshelman, A. L., and Meriwether, H. D., Report 4650. McDonnell-Douglas Aircraft Company, Inc., Santa Monica, Calif., 1967.
12. Slater, J. C., *J. Chem. Phys.*, Vol. 41, p. 3199, 1964.
13. Pauling, L., *J. Am. Chem. Soc.*, Vol. 69, p. 542, 1947.
14. Biedl, A., *Z. Kristallogr.* (to be published).
15. Haszko, S. E., *Trans. AIME*, Vol. 221, p. 201, 1961.
16. Brewer, L., Sawyer, D. L., Templeton, D. H., and Dagen, C., *J. Am. Ceram. Soc.*, Vol. 34, p. 173, 1951.